Radiology

Is Apparent Diffusion Coefficient Associated with Clinical Risk Scores for Prostate Cancers that Are Visible on 3-T MR Images?[1]

Baris Turkbey, MD
Vijay P. Shah, PhD
Yuxi Pang, PhD
Marcelino Bernardo, BS
Sheng Xu, PhD
Jochen Kruecker, PhD
Julia Locklin, RN
Angelo A. Baccala, Jr, MD
Ardeshir R. Rastinehad, DO
Maria J. Merino, MD
Joanna H. Shih, PhD
Bradford J. Wood, MD
Peter A. Pinto, MD
Peter L. Choyke, MD

Purpose: To investigate whether apparent diffusion coefficients (ADCs) derived from diffusion-weighted (DW) magnetic resonance (MR) imaging at 3 T correlate with the clinical risk of prostate cancer in patients with tumors that are visible on MR images, with MR imaging/transrectal ultrasonography (US) fusion–guided biopsy as a reference.

Materials and Methods: Forty-eight consecutive patients (median age, 60 years; median serum prostate-specific antigen value, 6.3 ng/mL) who underwent DW imaging during 3-T MR imaging with an endorectal coil were included in this retrospective institutional review board–approved study, and informed consent was obtained from each patient. Patients underwent targeted MR imaging/transrectal US fusion–guided prostate biopsy. Mean ADCs of cancerous target tumors were correlated with Gleason and D'Amico clinical risk scores. The true risk group rate and predictive value of the mean ADC for classifying a tumor by its D'Amico clinical risk score was determined by using linear discriminant and receiver operating characteristic analyses.

Results: A significant negative correlation was found between mean ADCs of tumors in the peripheral zone and their Gleason scores ($P = .003$; Spearman $\rho = -0.60$) and D'Amico clinical risk scores ($P < .0001$; Spearman $\rho = -0.69$). ADC was found to distinguish tumors in the peripheral zone with intermediate to high clinical risk from those with low clinical risk with a correct classification rate of 0.73.

Conclusion: There is a significant negative correlation between ADCs and Gleason and D'Amico clinical risk scores. ADCs may therefore be useful in predicting the aggressiveness of prostate cancer.

Supplemental material: *http://radiology.rsna.org/lookup/suppl/doi:10.1148/radiol.10100667/-/DC1*

[1] From the Molecular Imaging Program (B.T., V.P.S., M.B., P.L.C.), Center for Interventional Oncology (J.L., B.J.W.), Department of Radiology and Imaging Sciences, Clinical Center (J.L., B.J.W.), Urologic Oncology Branch (A.A.B., A.R.R., P.A.P.), Laboratory of Pathology (M.J.M.), and Biometric Research Branch, Division of Cancer Treatment and Diagnosis (J.H.S.), National Cancer Institute, National Institutes of Health, 10 Center Dr, MSC 1182, Bldg 10, Room B3B69F, Bethesda, MD 20892-1088; SAIC-Frederick, National Cancer Institute at Frederick, Frederick, Md (V.P.S., M.B.); Philips Healthcare, Cleveland, Ohio (Y.P.); and Philips Research North America, New York, NY (S.X., J.K.). Received March 30, 2010; revision requested June 2; revision received July 15; accepted August 13; final version accepted August 31. **Address correspondence to** P.L.C. (e-mail: *pchoyke@mail.nih.gov*).

Prostate cancer is the most common solid organ cancer among men in the western world, affecting approximately one in every six men. It is the second leading cause of cancer-related deaths in American men (1). Prostate cancer exists as a spectrum of disease that ranges from indolent to highly aggressive. Patients with indolent cancers may not require radical prostatectomy or radiation therapy, from which they would be at risk for side effects. Various methods of stratifying prostate cancers by risk categories have been devised, including pathologic stage, prognosis, and most notably, nomograms that incorporate laboratory findings (eg, serum prostate-specific antigen [PSA] values), demographics (eg, age), and physical findings (eg, digital rectal examination) (2–5). Whole-gland treatments, such as radical prostatectomy and radiation therapy, are offered for patients with intermediate to high clinical risk, whereas active surveillance is often suggested for patients with low volume and clinically low-risk disease (6).

Imaging offers a potentially important personalized prognostic indicator for prostate cancer (7–17). Diffusion-weighted (DW) magnetic resonance (MR) imaging and the calculated apparent diffusion coefficient (ADC), in particular, have been used to assess tumor aggressiveness in breast and brain cancers (18,19). The results of several trials with MR imaging suggest that it may be used to subclassify tumors according to aggressiveness on the basis of cell density, proliferation index, and histologic findings; however, little emphasis has been placed on the correlation of the ADC with Gleason and clinical risk scores (20–25). Since DW MR imaging is dependent on Brownian motion of water in biologic tissues, it is sensitive to the restricted diffusion that occurs in tumors owing to increased cellularity and fibrosis (26). Thus, ADCs may be helpful in assessing the aggressiveness of prostate cancer lesions. In this study, we investigate whether ADCs derived from DW MR imaging at 3 T correlate with the clinical risk scores of prostate cancer in patients with tumors that are visible on MR images.

Advance in Knowledge

- A significant negative correlation was found between mean apparent diffusion coefficients (ADCs) of prostate cancers in the peripheral zone and their Gleason ($P = .003$; Spearman $\rho = -0.60$) and D'Amico clinical risk ($P < .0001$; Spearman $\rho = -0.69$) scores.

Materials and Methods

Y.P., S.X., and J.K. are employees of Philips. B.J.W., P.A.P., and P.L.C. have a cooperative research and development agreement with Philips Healthcare (Best, the Netherlands). Philips holds intellectual property and has financial interests in the technology presented in this article. S.X., J.K., B.J.W., P.A.P., and P.L.C. hold intellectual property in the field of fusion biopsy.

Study Design and Patient Population

Our retrospective single-institution study was approved by the institutional review board of the National Cancer Institute at the National Institutes of Health and was compliant with the Health Insurance Portability and Accountability Act. Informed consent was obtained from each patient. Within a 2-year period, 260 patients underwent prostate MR imaging at 3 T. Among these patients, 48 consecutive patients underwent targeted MR imaging/transrectal ultrasonography (US) fusion–guided prostate biopsy with a positive result for tumor, and these patients were included in the study population. Patients who did not undergo MR imaging/transrectal US fusion–guided biopsy and patients who had a negative result for tumor were excluded from the study population. In the 48 patients who were included in our study, the median age was 60 years (mean, 62.6 years; range, 48–81 years), and the median serum PSA value was 6.3 ng/mL (mean, 8.28 ng/mL; range, 1.8–45 ng/mL).

Implication for Patient Care

- ADCs derived from 3-T diffusion-weighted MR images can be useful in the assessment of the aggressiveness of prostate cancer, which is important for patient treatment.

MR Imaging

MR imaging was performed by using a combination of an endorectal coil (BPX-30; Medrad, Pittsburgh, Pa) and a six-channel cardiac SENSE coil (Philips Healthcare) with a 3-T magnet (Achieva; Philips Healthcare) without prior bowel preparation. After digital rectal examination, the endorectal coil was inserted while the patient was in the left lateral decubitus position. A semianesthetic gel (lidocaine; AstraZeneca, Wilmington, Del) was used. The balloon surrounding the coil was distended with perfluorocarbon (Fluorinert FC-770; 3M, St. Paul, Minn) to a volume of approximately 50 mL. Axial, coronal, and sagittal T2-weighted MR images and axial DW MR images with five evenly spaced b values were obtained with the parameters summarized in Table 1. Images were obtained with

Published online before print
10.1148/radiol.10100667

Radiology 2011; 258:488–495

Abbreviations:
ADC = apparent diffusion coefficient
CG = central gland
DW = diffusion weighted
PSA = prostate-specific antigen
PZ = peripheral zone

Author contributions:
Guarantors of integrity of entire study, B.T., V.P.S., J.H.S., P.L.C.; study concepts/study design or data acquisition or data analysis/interpretation, all authors; manuscript drafting or manuscript revision for important intellectual content, all authors; approval of final version of submitted manuscript, all authors; literature research, B.T., V.P.S., A.R.R.; clinical studies, B.T., V.P.S., M.B., S.X., J.K., J.L., A.A.B., A.R.R., M.J.M., B.J.W., P.A.P., P.L.C.; statistical analysis, V.P.S., S.X., J.H.S., P.L.C.; and manuscript editing, B.T., V.P.S., Y.P., M.B., A.A.B., A.R.R., M.J.M., J.H.S., B.J.W., P.A.P.

Funding:
B.T., V.P.S., M.B., J.L., A.A.B., A.R.R., M.J.M., J.H.S., B.J.W., P.A.P., and P.L.C. are employees of the National Cancer Institute at the National Institutes of Health.

See Materials and Methods for pertinent disclosures.

Table 1

MR Imaging Parameters

Sequence	Repetition Time (msec)	Echo Time (msec)	Field of View (mm)	Resolution (mm)	Matrix	Flip Angle (degrees)	Section Thickness (mm)
T2-weighted turbo spin-echo							
Sagittal	2340	120	140	0.46 × 0.6 × 3.0	304 × 234	90	3
Axial	8852	120	140	0.46 × 0.6 × 3.0	304 × 234	90	3
Coronal	2340	120	140	0.46 × 0.58 × 3.0	304 × 242	90	3
Axial DW*	4140	57	160	1.25 × 1.29 × 3.0	112 × 108	90	3

* Twenty sections were obtained with five evenly spaced *b* values (ie, 0, 188, 375, 563, and 750 sec/mm^2).

Figure 1

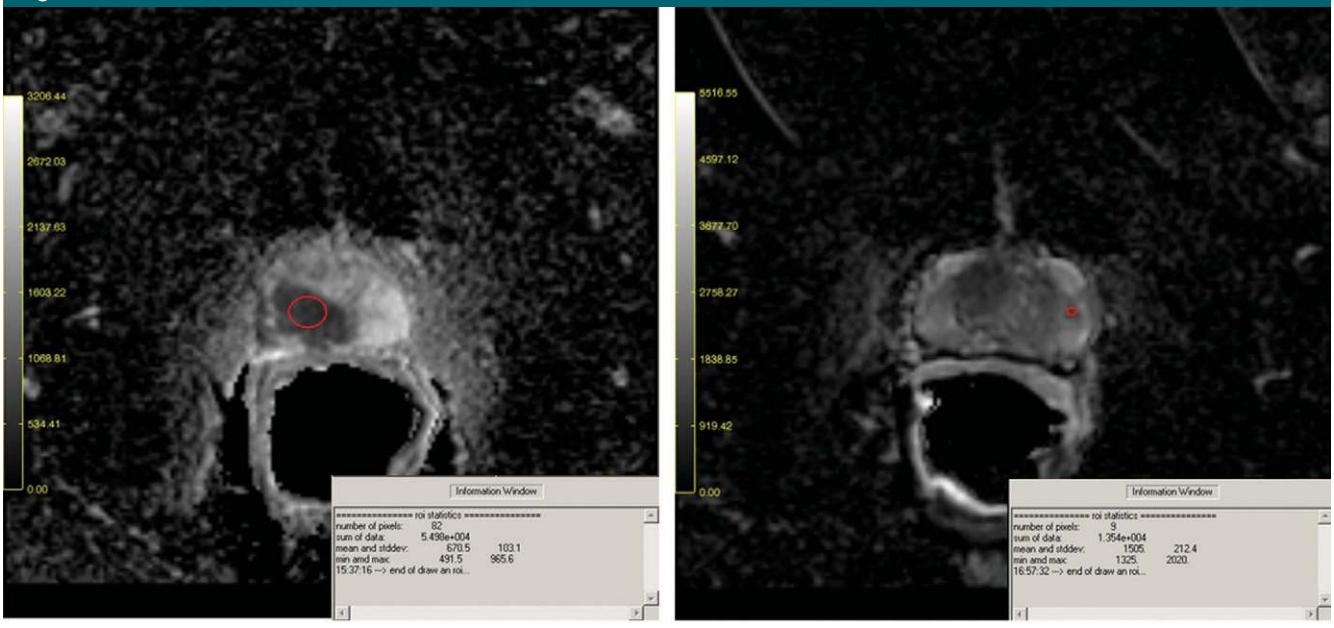

a. b.

Figure 1: Screen captures of the DW MR imaging tool used for analysis. **(a)** Region of interest (red) in a tumor in the right peripheral zone (PZ) with a Gleason score of 4+4 has a mean ADC of (670.5 ± 103.1) × 10^{-6} mm^2/sec, whereas **(b)** that in a tumor in the anterior left of the prostate with a Gleason score of 3+3 has a mean ADC of (1505 ± 212.4) × 10^{-6} mm^2/sec.

additional sequences (MR spectroscopy and dynamic contrast agent–enhanced MR imaging), but the results were not relevant to our study.

ADC maps were obtained by using linear least squares curve fitting of pixels (in log scale) in the five DW images against their corresponding *b* values following the simple monoexponential decay model. The following equation was used: $S = S_0 \times \exp(-b \times \text{ADC})$, where S and S_0 are the pixel value with DW gradients applied and that without, respectively, and b is the DW factor of the applied gradients. No attempt was made to separate the pseudodiffusion effects of random blood flow in microcapillaries from the true diffusion processes. ADC maps were created by using software developed in-house (IDL 6.4; ITTVIS, Boulder, Colo).

Target lesions for MR imaging/transrectal US fusion–guided biopsies were identified on T2-weighted MR images and ADC maps of DW MR images. The criterion for a positive lesion was a well-circumscribed or irregularly contoured round- or ellipsoid-shaped low-signal-intensity lesion within the prostate gland (27). MR imaging/transrectal US fusion–guided biopsies, as previously described (28,29), were performed in all patients. Two radiologists (B.T. and P.L.C., with 3 and 10 years experience in prostate MR imaging, respectively), who were blinded to the histologic findings, placed regions of interest that covered approximately 80% of each target lesion on a single image on each ADC map in consensus (median size, 14.5 mm^2; mean size, 12.5 mm^2; range, 2.4–41.5 mm^2). Analysis was performed by using a DW imaging toolkit developed in-house by using Interactive Data Language (version 6.4) (Fig 1).

Statistical Analysis

Mean ADCs of the target lesions that had positive tumor findings were compared with those of lesions with negative findings. Then, mean ADCs of target lesions with positive tumor findings were examined for correlation with Gleason scores. A clinical classification of the tumors that accounts for both Gleason score and serum PSA, known as the D'Amico clinical risk score, was also performed for each tumor (low: Gleason score $\leq$ 6 and PSA $\leq$ 10 ng/mL; intermediate: Gleason score = 7 or PSA $>$ 10 ng/mL, but $\leq$ 20 ng/mL; high: Gleason score $\geq$ 8 or PSA $>$ 20 ng/mL) (2,4). To account for intrapatient correlation between ADCs of multiple tumors, a linear mixed-effect model was used to estimate the differences of ADCs with respect to Gleason score and D'Amico clinical risk score. Analysis was performed for all tumors regardless of location, as well as separately for tumors located in either the PZ or central gland (CG).

Linear discriminant analysis was performed to assess the true risk group rate and the predictive value of ADC in classifying a tumor by its D'Amico clinical risk score, where true risk group rate was defined as correct assessment of the clinical risk score by ADC value. An additional linear discriminant analysis was performed after combining lesions with intermediate and high D'Amico clinical risk scores into one subgroup (eg, low vs intermediate and high). The linear discriminant analysis we used is an extension of traditional discriminant analysis that allows the number of classes to be greater than two. With a single predictor, it constructs a linear function based on the frequency of a class in log scale and squared z score for the difference of the value from the class mean. It assigns a case to a class if the squared z score minus twice the log frequency in that class is minimized (30,31). The leave-one-out cross-validation procedure was used to determine the true risk group rate and predictive value of the ADC for determining different subgroups (32). Receiver operating characteristic technique was used to assess different ADC thresholds for differentiating low clinical risk tumors from intermediate and high clinical risk tumors. The 95% confidence intervals for the estimates of true risk group rate, predicted value, and correct classification rate were constructed by using the bootstrap percentile method (limits are 2.5 and 97.5 percentiles of the bootstrap distribution) (33).

Table 2

Tumor Characteristics

	Gleason Score					D'Amico Clinical Risk Score			
Site	6	7	8	9	10	Low	Intermediate	High	Total
PZ	25	23	7	7	1	22	20	21	63
CG	2	6	3	1	0	2	3	7	12
Total	27	29	10	8	1	24	23	28	75

Note.—Data are numbers of tumors.

Table 3

Mean ADCs According to Gleason and D'Amico Clinical Risk Scores

	Mean ADC ($\times 10^{-6}$ mm^2/sec)		
Group	All Tumors	Tumors in PZ	Tumors in CG
Gleason score			
6	1217.8 ± 306.3	1254.0 ± 286.3	765.5 ± 175.9
7	980.4 ± 259.6	996.2 ± 284.5	919.7 ± 124.8
8	897.5 ± 117.5	908.9 ± 124.0	870.8 ± 120.4
9	804.7 ± 149.4	801.5 ± 161.0	826.6
10	599.7	599.7	…
P value	.0015	.003	.56
D'Amico clinical risk score			
Low	1233.0 ± 320.7	1275.6 ± 297.4	765.5 ± 175.9
Intermediate	1080.5 ± 230.6	1095.6 ± 240.4	980.3 ± 136.3
High	817.0 ± 142.0	802.9 ± 154.6	859.4 ± 90.5
P value	< .0001	< .0001	.43

Note.—Data are means ± standard deviations.

Results

In 48 patients before biopsy, MR imaging revealed 124 target lesions (108 in PZ, 16 in CG) suspicious for prostate cancer. After MR imaging/transrectal US fusion–guided biopsy, 75 target lesions were histologically confirmed as prostate cancer. Table 2 summarizes the tumor characteristics. The mean ADC for targeted tumors with positive biopsy findings ([1031 ± 294] $\times$ 10^{-6} mm^2/sec) was significantly lower than that for tumors with negative biopsy findings ([1293 ± 191] $\times$ 10^{-6} mm^2/sec) ($P < .0001$). The difference between mean ADC for low, intermediate, and high D'Amico clinical risk score tumors was significant ($P < .0001$) for all tumors (ie, those in PZ or CG) and tumors in the PZ only (Table 3; Figs 2, 3). The correct classification rate of ADC for D'Amico clinical risk score (low vs intermediate vs high) was 0.6 (Table E1 [online]). When the intermediate and high D'Amico clinical risk scores (low vs intermediate and high) were combined, the correct classification rate increased to 0.75 for all tumors; whereas the correct classification rate for PZ tumors was 0.73 (Table 4). Linear discriminant analysis results were not obtained for CG target lesions because the sample size (n = 12) was too small. On the basis of receiver operating characteristic

Figure 2

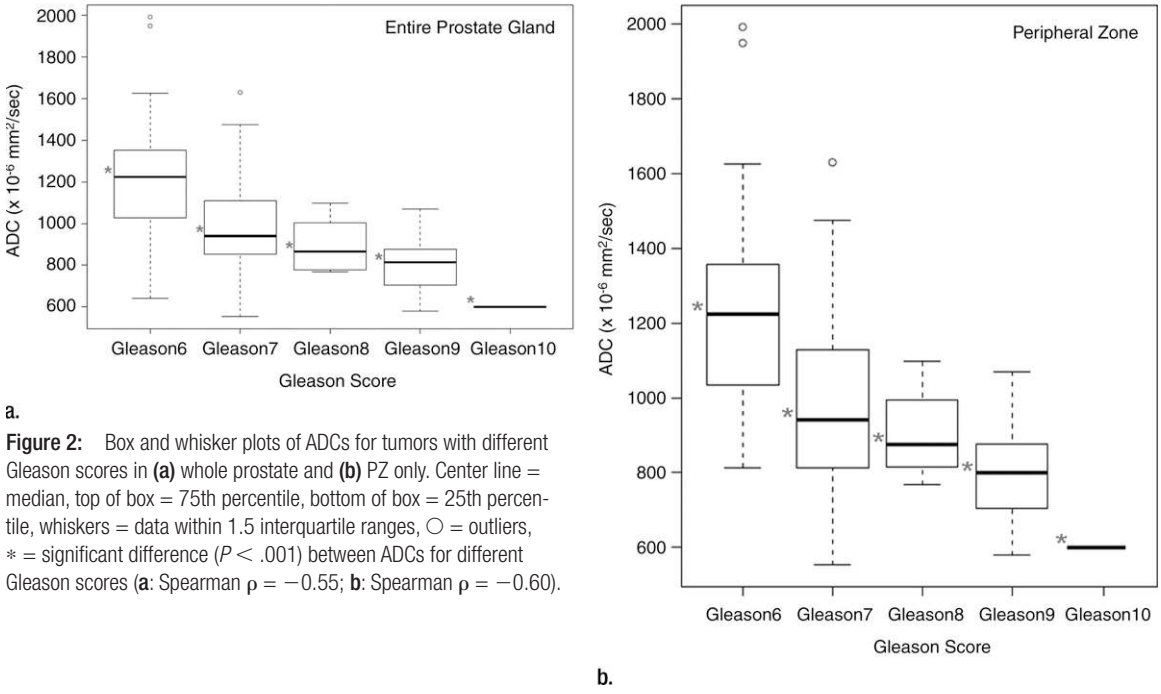

Figure 2: Box and whisker plots of ADCs for tumors with different Gleason scores in **(a)** whole prostate and **(b)** PZ only. Center line = median, top of box = 75th percentile, bottom of box = 25th percentile, whiskers = data within 1.5 interquartile ranges, ○ = outliers, * = significant difference ($P < .001$) between ADCs for different Gleason scores (**a**: Spearman $\rho = -0.55$; **b**: Spearman $\rho = -0.60$).

Figure 3

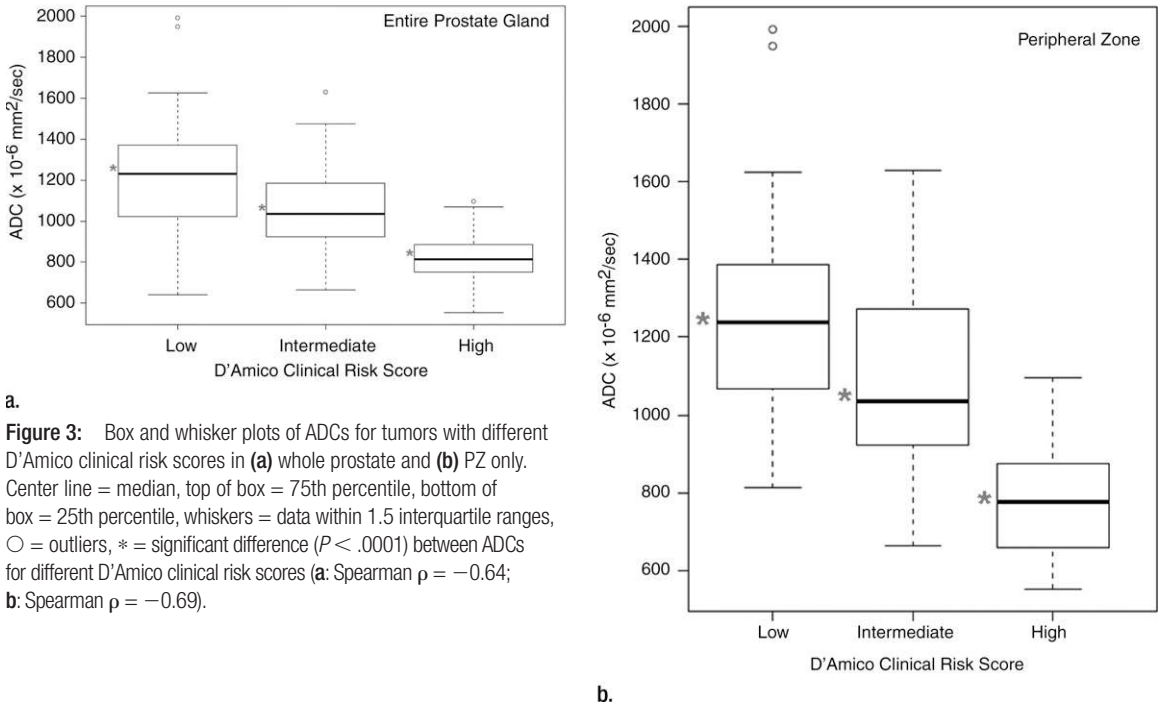

Figure 3: Box and whisker plots of ADCs for tumors with different D'Amico clinical risk scores in **(a)** whole prostate and **(b)** PZ only. Center line = median, top of box = 75th percentile, bottom of box = 25th percentile, whiskers = data within 1.5 interquartile ranges, ○ = outliers, * = significant difference ($P < .0001$) between ADCs for different D'Amico clinical risk scores (**a**: Spearman $\rho = -0.64$; **b**: Spearman $\rho = -0.69$).

Table 4

Predictive Value of ADC for D'Amico Clinical Risk Subgroups by Tumor Location

Parameter	D'Amico Clinical Risk Score: Low Risk	Intermediate and High Risk	Predictive Value*
	All Tumors		
ADC			
Low risk	10	5	0.67 (0.36, 0.92)
Intermediate and high risk	14	46	0.77 (0.60, 0.90)
True risk group rate*	0.42 (0.13, 0.68)	0.90 (0.82, 0.98)	
	Tumors in PZ		
ADC			
Low risk	10	5	0.67 (0.38, 0.91)
Intermediate and high risk	12	36	0.75 (0.57, 0.90)
True risk group rate*	0.45 (0.21, 0.75)	0.88 (0.77, 0.96)	

Note.—Unless otherwise specified, data are numbers of tumors. Overall mean correct classification rates are 0.75 (95% confidence interval: 0.61, 0.87) and 0.73 (95% confidence interval: 0.59, 0.87) for all tumors and tumors in PZ, respectively.

* Data are means, with 95% confidence intervals in parentheses.

Figure 4

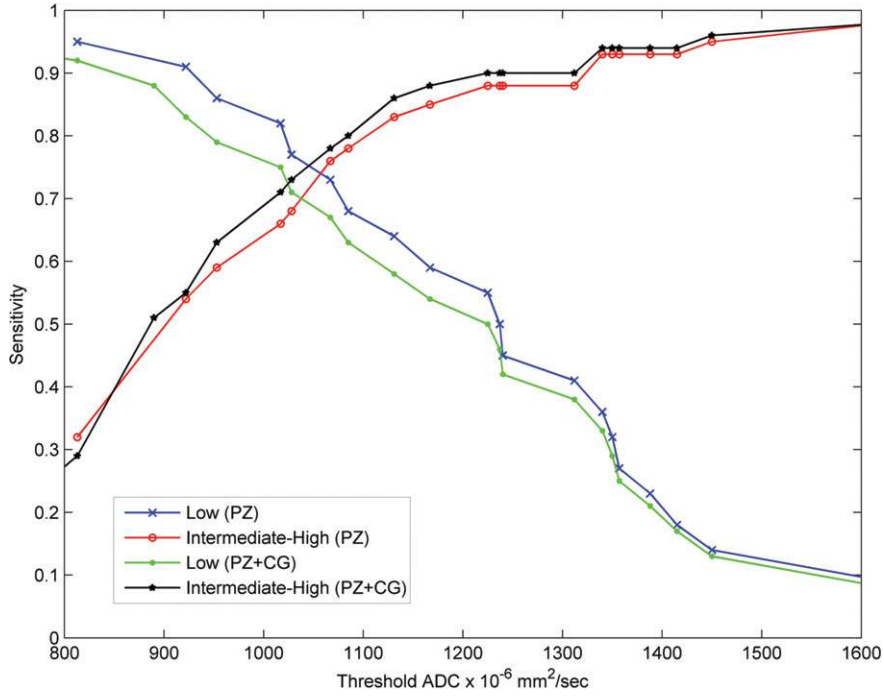

Figure 4: True risk group rate *(Sensitivity)* of different threshold ADCs for determining low versus intermediate to high *(Intermediate-High)* D'Amico clinical risk scores in all tumors *(PZ+CG)* and tumors only in the PZ.

analysis, a threshold of 1067.4×10^{-6} mm^2/sec for ADC was found to result in a 78% chance of correctly detecting a tumor as intermediate or high clinical risk for overall tumors and a 76% chance of the same for PZ tumors (Fig 4).

Discussion

Gleason score is the most commonly accepted and widely used system for evaluating the aggressiveness of prostate cancer. The D'Amico clinical risk score has been introduced to provide a more accurate assessment of tumor aggressiveness by combining the Gleason score with the serum PSA value (2,4).

In our study, the mean ADC of tumors had a significant negative correlation with tumor Gleason scores. Possible explanations to this could be increased tumor cellularity, structural change of gland stroma that becomes more fibrous, and a more disorganized texture resulting in a relatively more restricted motion of water molecules within high Gleason score tumors. Moreover, a significant difference was also observed between mean ADCs of low, intermediate, and high clinical risk tumors (2,4). This is consistent with the results of Tamada et al (23) who reported a negative correlation between ADCs and Gleason scores of PZ tumors in 90 patients with prostate cancer who underwent 1.5-T MR imaging. Mazaheri et al (34) and deSouza et al (25) compared ADCs for low- versus high-risk prostate cancers and similarly demonstrated significant differences between the two groups at 1.5 T. Van As et al (35) reported that the ADC of a single Gleason 4+5 tumor was significantly lower than that of 10 other tumors in the study that were graded as either Gleason 6 or 7. Additionally, several studies have reported a correlation between ADCs and tumor cellular density and proliferation; however, the majority of these studies focused on differentiating tumors from normal prostate for diagnostic purposes (22,24,36,37).

Determining biologic aggressiveness has implications for patient treatment. The decision to undergo active surveillance is based on several factors, including serum PSA, PSA velocity, PSA density, Gleason score, and percentage or number of positive cores. Active surveillance is most appropriate in patients with low clinical risk, although some intermediate clinical risk patients elect this strategy (38–42). We observed that ADC maps can be used to assess the aggressiveness of a prostate cancer lesion, potentially as an adjunct to information from other clinical sources (eg, Gleason score, PSA, lesion size, lesion stage) to help select patients who are

most appropriate for active surveillance. Moreover, ADC maps can be used to follow changes in tumor aggressiveness in patients undergoing active surveillance in the interval, since ADC maps are repeatable and reproducible (43). This can provide a noninvasive way to follow these patients as compared with repeated biopsy.

Our study had several limitations. First, our analysis was retrospective and only abnormal areas depicted on T2-weighted MR images and ADC maps were evaluated. Thus, there may have been a selection bias against lesions that were not depicted on T2-weighted MR images and ADC maps. Second, results from MR imaging-transrectal US fusion–guided biopsy were used as the reference standard for validation instead of whole-mount histopathologic maps; however, this system has been found to be accurate (2.4 mm ± 1.2) in phantom and canine studies (29). Additionally, although the box and whisker plots demonstrate a substantial overlap in ADCs of different Gleason scores and D'Amico clinical risk scores, our statistical analysis indicates that ADCs can be used to differentiate tumors with higher Gleason scores and intermediate to high clinical risk scores from those with lower scores. Finally, our study population, the number of tumors analyzed, and the number of tumors with higher (≥8) Gleason scores are relatively small, reflecting the distribution of Gleason score in a screened population in the United States. Larger prospectively studied patient populations will be needed to refine the cutoff values and the relationship between ADCs and tumor aggressiveness.

In conclusion, ADCs obtained from DW MR imaging at 3 T were significantly lower in prostate cancers with intermediate and high clinical risk scores and higher Gleason scores. This finding may be useful in the noninvasive assessment of the aggressiveness of prostate cancers that are visible on MR images, which is an important predictor for patient outcome and prognosis and may aid in selecting and following up patients who are most appropriate for active surveillance.

References

1. American Cancer Society. Cancer facts & figures 2009. Atlanta, Ga: American Cancer Society, 2009.
2. D'Amico AV, Whittington R, Malkowicz SB, et al. Biochemical outcome after radical prostatectomy, external beam radiation therapy, or interstitial radiation therapy for clinically localized prostate cancer. JAMA 1998;280(11):969–974.
3. Partin AW, Mangold LA, Lamm DM, Walsh PC, Epstein JI, Pearson JD. Contemporary update of prostate cancer staging nomograms (Partin Tables) for the new millennium. Urology 2001;58(6):843–848.
4. D'Amico AV, Moul J, Carroll PR, Sun L, Lubeck D, Chen MH. Cancer-specific mortality after surgery or radiation for patients with clinically localized prostate cancer managed during the prostate-specific antigen era. J Clin Oncol 2003;21(11):2163–2172.
5. Stephenson AJ, Scardino PT, Eastham JA, et al. Preoperative nomogram predicting the 10-year probability of prostate cancer recurrence after radical prostatectomy. J Natl Cancer Inst 2006;98(10):715–717.
6. Bill-Axelson A, Holmberg L, Ruutu M, et al. Radical prostatectomy versus watchful waiting in early prostate cancer. N Engl J Med 2005;352(19):1977–1984.
7. Kim CK, Park BK, Kim B. Localization of prostate cancer using 3T MRI: comparison of T2-weighted and dynamic contrast-enhanced imaging. J Comput Assist Tomogr 2006;30(1):7–11.
8. Park BK, Kim B, Kim CK, Lee HM, Kwon GY. Comparison of phased-array 3.0-T and endorectal 1.5-T magnetic resonance imaging in the evaluation of local staging accuracy for prostate cancer. J Comput Assist Tomogr 2007;31(4):534–538.
9. Fütterer JJ, Heijmink SW, Scheenen TW, et al. Prostate cancer localization with dynamic contrast-enhanced MR imaging and proton MR spectroscopic imaging. Radiology 2006;241(2):449–458.
10. Ocak I, Bernardo M, Metzger G, et al. Dynamic contrast-enhanced MRI of prostate cancer at 3 T: a study of pharmacokinetic parameters. AJR Am J Roentgenol 2007;189(4):W192–W201.
11. Fütterer JJ, Engelbrecht MR, Huisman HJ, et al. Staging prostate cancer with dynamic contrast-enhanced endorectal MR imaging prior to radical prostatectomy: experienced versus less experienced readers. Radiology 2005;237(2):541–549.
12. Kurhanewicz J, Vigneron DB, Hricak H, Narayan P, Carroll P, Nelson SJ. Three-dimensional H-1 MR spectroscopic imaging of the in situ human prostate with high (0.24-0.7-cm3) spatial resolution. Radiology 1996;198(3):795–805.
13. Casciani E, Polettini E, Bertini L, et al. Contribution of the MR spectroscopic imaging in the diagnosis of prostate cancer in the peripheral zone. Abdom Imaging 2007;32:796–802.
14. Westphalen AC, Coakley FV, Qayyum A, et al. Peripheral zone prostate cancer: accuracy of different interpretative approaches with MR and MR spectroscopic imaging. Radiology 2008;246(1):177–184.
15. Villers A, Puech P, Mouton D, Leroy X, Ballereau C, Lemaitre L. Dynamic contrast enhanced, pelvic phased array magnetic resonance imaging of localized prostate cancer for predicting tumor volume: correlation with radical prostatectomy findings. J Urol 2006;176(6 pt 1):2432–2437.
16. Yu KK, Scheidler J, Hricak H, et al. Prostate cancer: prediction of extracapsular extension with endorectal MR imaging and three-dimensional proton MR spectroscopic imaging. Radiology 1999;213(2):481–488.
17. Riches SF, Payne GS, Morgan VA, et al. MRI in the detection of prostate cancer: combined apparent diffusion coefficient, metabolite ratio, and vascular parameters. AJR Am J Roentgenol 2009;193(6):1583–1591.
18. Guo Y, Cai YQ, Cai ZL, et al. Differentiation of clinically benign and malignant breast lesions using diffusion-weighted imaging. J Magn Reson Imaging 2002;16(2):172–178.
19. Sugahara T, Korogi Y, Kochi M, et al. Usefulness of diffusion-weighted MRI with echo-planar technique in the evaluation of cellularity in gliomas. J Magn Reson Imaging 1999;9(1):53–60.
20. Wang L, Mazaheri Y, Zhang J, Ishill NM, Kuroiwa K, Hricak H. Assessment of biologic aggressiveness of prostate cancer: correlation of MR signal intensity with Gleason grade after radical prostatectomy. Radiology 2008;246(1):168–176.
21. Zakian KL, Sircar K, Hricak H, et al. Correlation of proton MR spectroscopic imaging with Gleason score based on step-section pathologic analysis after radical prostatectomy. Radiology 2005;234(3):804–814.
22. Wang XZ, Wang B, Gao ZQ, et al. Diffusion-weighted imaging of prostate cancer: correlation between apparent diffusion coefficient values and tumor proliferation. J Magn Reson Imaging 2009;29(6):1360–1366.

23. Tamada T, Sone T, Jo Y, et al. Apparent diffusion coefficient values in peripheral and transition zones of the prostate: comparison between normal and malignant prostatic tissues and correlation with histologic grade. J Magn Reson Imaging 2008;28(3):720–726.

24. Zelhof B, Pickles M, Liney G, et al. Correlation of diffusion-weighted magnetic resonance data with cellularity in prostate cancer. BJU Int 2009;103(7):883–888.

25. deSouza NM, Riches SF, Vanas NJ, et al. Diffusion-weighted magnetic resonance imaging: a potential non-invasive marker of tumour aggressiveness in localized prostate cancer. Clin Radiol 2008;63(7):774–782.

26. Padhani AR, Liu G, Koh DM, et al. Diffusion-weighted magnetic resonance imaging as a cancer biomarker: consensus and recommendations. Neoplasia 2009;11(2):102–125.

27. Heijmink SW, Fütterer JJ, Hambrock T, et al. Prostate cancer: body-array versus endorectal coil MR imaging at 3 T—comparison of image quality, localization, and staging performance. Radiology 2007;244(1):184–195.

28. Singh AK, Kruecker J, Xu S, et al. Initial clinical experience with real-time transrectal ultrasonography-magnetic resonance imaging fusion-guided prostate biopsy. BJU Int 2008;101(7):841–845.

29. Xu S, Kruecker J, Turkbey B, et al. Real-time MRI-TRUS fusion for guidance of targeted prostate biopsies. Comput Aided Surg 2008;13(5):255–264.

30. Johnson RA, Wichern DW. Applied multivariate statistical analysis. 5th ed. Englewood Cliffs, NJ: Prentice Hall, 2002.

31. R Development Core Team. R: a language and environment for statistical computing. Vienna, Austria: R Foundation for Statistical Computing, 2009.

32. Kohavi R, Provost F. Glossary of terms. Mach Learn 1998;30(2-3):271–274.

33. Efron B, Tibshirani RJ. An introduction to the bootstrap. Boca Raton, Fla: Chapman & Hall/CRC, 1993.

34. Mazaheri Y, Hricak H, Fine SW, et al. Prostate tumor volume measurement with combined T2-weighted imaging and diffusion-weighted MR: correlation with pathologic tumor volume. Radiology 2009;252(2):449–457.

35. Van As N, Charles-Edwards E, Jackson A, et al. Correlation of diffusion-weighted MRI with whole mount radical prostatectomy specimens. Br J Radiol 2008;81(966):456–462.

36. Gibbs P, Liney GP, Pickles MD, Zelhof B, Rodrigues G, Turnbull LW. Correlation of ADC and T2 measurements with cell density in prostate cancer at 3.0 Tesla. Invest Radiol 2009;44(9):572–576.

37. Woodfield CA, Tung GA, Grand DJ, Pezzullo JA, Machan JT, Renzulli JF 2nd. Diffusion-weighted MRI of peripheral zone prostate cancer: comparison of tumor apparent diffusion coefficient with Gleason score and percentage of tumor on core biopsy. AJR Am J Roentgenol 2010;194(4):W316–W322.

38. Klotz LH. Active surveillance for good risk prostate cancer: rationale, method, and results. Can J Urol 2005;12(suppl 2):21–24.

39. Roemeling S, Roobol MJ, Postma R, et al. Management and survival of screen-detected prostate cancer patients who might have been suitable for active surveillance. Eur Urol 2006;50(3):475–482.

40. Dall'Era MA, Konety BR, Cowan JE, et al. Active surveillance for the management of prostate cancer in a contemporary cohort. Cancer 2008;112(12):2664–2670.

41. Ercole B, Marietti SR, Fine J, Albertsen PC. Outcomes following active surveillance of men with localized prostate cancer diagnosed in the prostate specific antigen era. J Urol 2008;180(4):1336–1339.

42. van den Bergh RC, Roemeling S, Roobol MJ, et al. Gleason score 7 screen-detected prostate cancers initially managed expectantly: outcomes in 50 men. BJU Int 2009;103(11):1472–1477.

43. Gibbs P, Pickles MD, Turnbull LW. Repeatability of echo-planar-based diffusion measurements of the human prostate at 3 T. Magn Reson Imaging 2007;25(10):1423–1429.